Initial spindle formation at the oocyte center protects against incorrect kinetochore-microtubule attachment and aneuploidy in mice

Jessica N. Kincade and Ahmed Z. Balboula

Animal Sciences Research Center, University of Missouri, Columbia, MO 65211, USA

Running title: Spindle formation centrally protects against aneuploidy

Keywords: Aneuploidy, GV Positioning, Spindle Positioning, Oocyte, Meiosis

*Corresponding author: Ahmed Z. Balboula, Animal Sciences Research Center, University of Missouri, Columbia, MO 65211, USA, abalboula@missouri.edu

ABSTRACT

Aneuploidy is the leading genetic cause of miscarriage and infertility in women and occurs frequently in oocytes. Spindle formation and positioning are two critical events that must be regulated tightly to avoid erroneous chromosome segregation. Following nuclear envelope breakdown (NEBD), the spindle is assembled centrally before migrating towards the cortex to allow the first asymmetric division. The biological significance of the primary central positioning of the spindle is unknown. Because the spindle forms where NEBD occurs, whether positioned at the center or at the cortex of the cell, full-grown GV (prophase I) oocytes were collected from CF-1 mice (6-8 weeks old) and sorted according to the position of the GV into three groups: central, intermediate, and peripheral. Approximately 50% of the cells exhibited a central GV position, while 25% of cells showed a peripheral GV position. These proportions were similar to those obtained by histological evaluation of ovarian oocytes in 6-8 week mice, but not to those of mice aged less than 5 weeks, which tended to have a majority of peripherally positioned GVs. When peripheral GV oocytes were matured *in vitro*, GVs (88%) migrated towards the center and NEBD (and spindle assembly) occurred either at the center of the cell or during migration. The percentages of NEBD and polar body (PB) extrusion did not vary significantly among groups. Importantly, peripheral GV oocytes had a significant increase of abnormal K-MT attachments at metaphase I (Met I) and showed a significant increase of aneuploidy at metaphase II (Met II) when compared to central GV oocytes. Interestingly, peripheral GV oocytes that were able to achieve full GV relocation to the center were half as likely to experience aneuploidy when compared to peripheral GV oocytes unable to achieve relocation. These results indicate that preferential central spindle formation is an insurance mechanism to protect against incorrect K-MT attachments and aneuploidy.

INTRODUCTION

Infertility is an extremely prevalent issue worldwide, affecting approximately 122 million women worldwide (Sun, et al., 2019). The leading genetic cause of infertility is aneuploidy and can be characterized as errors within chromosomal segregation (Jacobs, et al., 1959, Lejeune, et al., 1959). Fertility and aneuploidy demonstrate an inversely correlated relationship throughout the lifetime of a female, with the highest incidence of aneuploidy occurring at the lowest rate of fertility (Gruhn, et al., 2019). Aneuploidy often causes failure to fertilize, miscarriage, spontaneous abortion, congenital defects *in vivo* (ex: down syndrome), and is the leading contributor to *in vitro* fertilization failure (Angell, et al., 1986, Byrne, et al., 1985, Gruhn, Zielinska, Shukla, Blanshard, Capalbo, Cimadomo, Nikiforov, Chan, Newnham, Vogel, Scarica, Krapchev, Taylor, Kristensen, Cheng, Ernst, Bjorn, Colmorn, Blayney, Elder, Liss, Hartshorne, Grondahl, Rienzi, Ubaldi, McCoy, Lukaszuk, Andersen, Schuh and Hoffmann, 2019, Hassold and Hunt, 2001). Aneuploidy more commonly arises in female gametes (eggs) than in male gametes (Hassold and Hunt, 2001), and from mistakes during Meiosis I (MI) than they do in MII (Hassold, et al., 2007). Therefore, as the average maternal age increases, so does the risk of infertility and aneuploidy; it is crucial to understand basic mechanisms regulating female meiosis I.

Oogenesis is a complex process that begins during fetal development in female mammalian species, shortly after conception. During the third trimester of pregnancy, oogonia enter meiosis I (MI) and duplicate their chromosomes (Gilbert, 2000). Shortly after birth, all germ cells undergo a prolonged arrest that is maintained until puberty. Hormonal stimulation during ovulation causes the oocytes to resume meiosis (Gilbert, 2000). In full-grown prophase I oocytes, the

germinal vesicle (GV) localizes mainly at the center (Brunet and Maro, 2007). *In vitro*, peripherally localized GV migrates towards the cortex, regulated by F-actin. The network of filamentous actin within the oocyte, more dense at the cortex and less dense at the center due to gradients of GTPases (Azoury, et al., 2008), relocates the GV centrally through gentle movement governed by active diffusion, rather than exerting a force on the GV (Almonacid, et al., 2015). However, why the GV relocates to the center of the oocyte remains unknown.

Upon meiotic resumption, prophase I oocytes undergo nuclear envelope breakdown (NEBD). Throughout the NEBD process, the microtubule organizing centers (MTOCs) undergo a three-step fragmentation before clustering and sorting into two dominant spindle poles that are integral in forming a bipolar spindle at the center of the oocyte in Met I (Schuh and Ellenberg, 2007). The spindle dictates the plane of cell division (McCarthy and Goldstein, 2006), and therefore must migrate to the cortex of the oocyte to ensure the highly asymmetric meiotic division (Longo and Chen, 1985, McCarthy and Goldstein, 2006). Extruding a small polar body through a highly asymmetrical division is critical as it allows the egg to retain a majority of the cytoplasmic store of maternal RNAs and proteins synthesized during the growth phase which are essential to fertilization and early embryonic development (Ma, et al., 2006, Menezo, 2006). Once again, however, the biological significance of primary central formation and positioning of the spindle prior to its cortical migration is unknown.

Given that the spindle forms where NEBD occurs (Balboula, et al., 2016, Balboula, et al., 2015), we sorted full-grown GV oocytes according to the positioning of the GV into three groups: central, intermediate, and peripheral. We used these models as a tool to study the biological significance of central spindle formation and positioning. Here we show that GV positioning is a

dynamic process that depends on maternal age, mice aged 6-8 weeks maintain a majority of centrally positioned GV oocytes, and that peripheral GV positioning is associated with increased chromosome misalignment, incorrect kinetochore-microtubule (K-MT) attachments and aneuploidy. Importantly, allowing peripherally positioned GV oocytes to relocate the GV to the center, significantly decreased the rate of aneuploidy. Our results are the first to demonstrate that preferential central spindle formation and its positioning at the center of the oocyte are critical to establish correct K-MT attachments and protect against aneuploidy in mammalian oocytes.

RESULTS

GV Positioning – A dynamic process

Because the spindle forms where NEBD occurs (Balboula, Nguyen, Gentilello, Quartuccio, Drutovic, Solc and Schindler, 2016, Balboula, Stein, Schultz and Schindler, 2015), we sorted full-grown GV oocytes according to the positioning of the GV into three groups: central, intermediate, and peripheral; from here out, these groups were referred to as containing central GV oocytes, intermediate GV oocytes, or peripheral GV oocytes (Fig. 1A). Peripheral GV oocytes had a distance of 5 μm or less from the GV to the nearest cortex, intermediate GV oocytes remained a distance of 5 to 15 μm from the GV to the nearest cortex, and central GV oocytes maintained more than 15 μm distance from the GV to the nearest cortex (Fig. 1A,B). First, we observed the proportions of these groups of oocytes *in vitro.* Oocytes with a centrally located germinal vesicle were the most prevalent, nearly 47.34% of all oocytes collected. Oocytes with intermediately positioned GV accounted for nearly 27.75% of all collected oocytes, while peripheral oocytes represented only 24.91% of collected cells (Fig. 1C,D).

To determine whether GV positioning proportions *in vitro* are similar to those *in vivo*, ovaries were collected at four ages (2 weeks, 3 weeks, 5 weeks, and 8 weeks) in order to display GV positioning throughout sexual development. All oocytes and their corresponding GV positioning were examined from histological sections of ovary stained with Hematoxylin and Eosin (Fig. 1E,F). Similar to our *in vitro* results, ovaries from mice aged 8 weeks showed a majority of oocytes with centrally positioned GVs (65.98%). Interestingly, younger mice (2 & 3 weeks of age) showed a majority of peripherally located GV (50.46% and 55.63%, respectively) respectively, while mice aged 5 weeks showed very similar proportions of oocytes with both centrally and peripherally located GVs (42.86% and 43.25%, respectively) (Figure 1.F,G), suggesting that, before sexual maturation, oocytes have eccentrically positioned GVs (likely incompetent) prior to their central relocation after sexual maturation.

Oocytes with cortically located GV associate with higher rates of chromosome misalignment and aneuploidy

Upon meiotic resumption, the germinal vesicle (GV) undergoes nuclear envelope breakdown (NEBD) and is shortly followed by the formation of a bipolar spindle and the alignment of chromosomes at the metaphase plate. Peripheral GV positioning increases with maternal age and correlates with decreased maturation rate (Brunet, 2007). To assess the meiotic progression, oocytes were collected from 6-8 weeks old mice and matured for 16 h (Met II). The majority (~92%) of centrally located GV oocytes were able to successfully undergo NEBD. On the other hand, peripherally located GV oocytes showed a significant decrease in the percentage of successful NEBD (~61%) (Figure 2A). However, using time-lapse microscopy, we found no significant difference in the timing of NEBD between centrally located GV oocytes and

peripherally located GV oocytes (Figure 2B). Similarly, a majority of centrally located GV oocytes were able to undergo successful polar body extrusion (PBE, ~81%), while peripherally located GV oocytes demonstrated a tendency to be less successful to extrude the first PB (~59%, Fig. 2C). Once again, there was no significant difference in the time of PBE when both centrally located GV oocytes and peripherally located GV oocytes were compared (Fig. 2D).

To assess the spindle morphology and chromosome alignment among the groups, oocytes were matured *in vitro* for either 7 h (Met I) or 16 h (Met II), fixed, and immunostained with α-tubulin to label the spindle and stained with DAPI to label the DNA. Interestingly, we found a significant increase in the percentage of chromosome misalignment either at Met I or Met II in oocytes with more peripherally positioned GV when compared to centrally located ones. Intermediate GV oocytes also showed significantly higher rates of chromosome misalignment when compared to central GV oocytes in Met I, but not at Met II (Fig. 2E,F,H,I). Chromosome alignment was assessed according to the parameters previously described by (Lane, et al., 2012). On the other hand, spindle morphology did not vary significantly among groups in both Met I and Met II oocytes (Fig. 2E,G,H,J). Because chromosome misalignment is highly associated with aneuploidy, we then assessed aneuploidy in Met II eggs using *in situ* chromosome counting. Strikingly, segregation errors occurred in oocytes with peripherally located GV (~50.15%) nearly 5 times more frequently than oocytes with a centrally located GV (~10.37%, Fig. 2K,L).

Nuclear envelope breakdown occurs during central relocation of peripherally located GV

To understand the behavior of the GV and its positioning within the meiotic process, we employed time-lapse microscopy to image the oocytes live every 10 min (Fig. 3A). Interestingly, the GV favors central movement prior to NEBD, as previously reported in (Almonacid, et al.,

2014, Sanfins, et al., 2003, Sanfins, et al., 2004). When peripheral GV oocytes were arrested at prophase I by milrinone, a phosphodiesterase inhibitor, only 12.33% of the oocytes remained peripheral after overnight incubation, while the majority (87.67%) relocated to the center of the oocyte (Fig. 3B). When the oocytes were allowed to mature in milrinone-free medium, chromosomes that were initially positioned more peripherally (GV) remained closer to the cortex than intermediately and centrally located ones at the time of chromosome misalignment (Fig. 3C). It is of note that the timing of chromosome misalignment did not vary significantly among groups (Fig. 3D). The distance from the GV to the nearest cortex was also measured at NEBD. Notably, the GV which was initially located at the peripheral of the cell underwent 10 ± 1.256 µm movement towards the center before the oocyte aligns its chromosomes. Intermediately located GV and centrally located GV underwent central movement and traveled a distance of 6 ± 0.6024 µm and 4 ± 0.6783 µm, respectively before chromosome alignment (Fig. 3E). Why oocytes favor central GV positioning is not yet known.

Incorrect kinetochore-microtubule attachments are increased in oocytes with peripherally located germinal vesicle

One important cause of aneuploidy is a weakened or non-functional spindle assembly checkpoint (SAC). Typically, the SAC is inactivated when microtubules are attached correctly to all kinetochores, but a weakened or non-functional SAC may allow the progression of the cell to anaphase and telophase without proper K-MT attachments, a phenomenon that is highly associated with aneuploidy. To assess the SAC function in oocytes with a central, intermediate, or peripheral GV, oocytes were treated with nocodazole, a MT depolymerizing agent that is known to maintain the SAC active and thereby prevent PBE by inducing Met I arrest.

Expectedly, positive control oocytes treated by ZM447439, an Aurora Kinase B/C inhibitor that is known to disrupt the SAC function at a high dose (10μM), extruded the PB even in the presence of nocodazole (Lane, et al., 2010). In contrast to ZM447439 treated oocytes, all oocytes (central, intermediate and peripheral) failed to extrude a PB in the presence of nocodazole, suggesting that the SAC is intact and functional (Fig. 4A).

Because improper K-MT attachment is another major contributor of aneuploidy and because cortically facing centromeres have relatively high rates of unstable K-MT attachments (Akera, et al., 2017), we hypothesized that early spindle formation and its positioning in the center of the oocyte is required to protect against a cortical influence that may hinder correct K-MT attachments. Even if the SAC is satisfied by KMT attachment, it is not necessary that all attachments are correct and homologous chromosomes are bioriented. To assess K-MT attachments, Met I oocytes were (~7 h) were exposed to a brief cold shock (6 minutes) to depolymerize liable unattached MTs and maintain stable MT fibers that are attached to kinetochores, immunostained, and imaged using confocal microscopy. An α-tubulin antibody was used to label MTs and CREST was used to label kinetochores. K-MT attachments were scored as normal, unattached, or abnormally attached (merotelic or syntelic) (Fig. 4B). GV positioning had no effect on the percentage of unattached kinetochores among all groups (Fig. 4B,C). Importantly, oocytes with peripherally located GV displayed ~ four-fold increase in the percentage of incorrect K-MT attachments, compared to oocytes with centrally located GV (Fig. 4B-D). Moreover, the percentages of peripheral (37.93 ± 9.17%) and intermediate (39.13 ± 10.41%) oocytes having two or more abnormally attached kinetochores were significantly higher than those in the central group (7.14 ± 4.02%). These results suggest that improper K-MT

attachments are the likely cause of increased aneuploidy in oocytes with a peripherally located GV (Fig. 4F).

Allowing for central GV relocation partially rescues chromosome mis-segregation

To confirm that the cortical influence during spindle formation is the cause, at least partially, of the high rate of aneuploidy in peripherally located GV oocytes, we tracked the movement of the GV live using time-lapse microscopy. Oocytes with a peripherally located GV demonstrated one of three types of movement: oocytes that were able to achieve complete relocation of the GV to the center were termed 'corrected', oocytes that demonstrated central movement prior to NEBD but did not achieve full relocation were termed 'migratory', and oocytes that failed to make a relocation attempt and remained at the cortex were termed 'peripheral' (Fig. 5A,B). Strikingly, oocytes that were able to successfully relocate their GVs to the center showed rates of aneuploidy similar to those of oocytes beginning with a central GV. On the other hand, oocytes that failed to attempt GV relocation and underwent NEBD at the periphery of the cell continued to experience high levels of aneuploidy, suggesting that the spindle must form and position at the center of the oocyte initially to avoid cortical influence detrimental to the fidelity of establishing K-MT attachments (Fig. 5C).

DISCUSSION

Spindle formation and its positioning are two critical events that must be regulated tightly to avoid erroneous chromosome segregation. Upon meiotic resumption and shortly after NEBD, the spindle is assembled and remains at the center of the oocyte prior to its migration towards the cortex. The biological significance of primary spindle formation and its positioning at the center

of the oocyte has not been studied. Prophase I oocytes were collected and sorted according to the position of the GV into three groups: central, intermediate, and peripheral. Here we show that the majority of oocytes in the ovaries of sexually mature mice (~ 6-8-weeks old) had a centrally localized GV, whereas mice aged less than 5 weeks had a majority of peripherally positioned GVs in their ovaries. Because the spindle is assembled where NEBD occurs, we took the advantage of the aforementioned observation and compared the consequences when the spindle is formed at the center (central GV oocyte), at the cortex (peripheral GV oocyte) or in between (intermediate GV oocyte). Although we did not find a significant difference in the rate of PBE among groups, peripheral GV oocytes showed a significant decrease in the percentage of NEBD and a significant increase in chromosome misalignment, abnormal K-MT attachments, and aneuploidy when compared to central GV oocytes. Importantly, peripheral GV oocytes that were able to relocate their GVs to the center showed significantly lower levels of aneuploidy when compared to peripheral GV oocytes that were unable to relocate their GVs to the center. These results suggest that primary spindle formation and its positioning in the center of the oocyte are critical to allow proper K-MT attachments and to prevent against the development of aneuploid gametes.

Abnormal K-MT attachments during Met I is a major cause of aneuploidy in mammalian oocytes (Lane, et al., 1999, Orr, et al., 2015). Our results that peripheral GV oocytes, in which the spindle formed and positioned near the cortex during prometaphase I, had significantly higher rates of abnormal K-MT attachments at Met I and aneuploidy at Met II when compared to those in central GV oocytes, suggest that the cortical signals may have an influence on the ability of the oocyte to establish correct K-MT attachments. Indeed, recent evidence suggests that cortical

signals have the capability to influence spindle asymmetry (Akera, Chmatal, Trimm, Yang, Aonbangkhen, Chenoweth, Janke, Schultz and Lampson, 2017). In addition, cortical polarization of the spindle (and following asymmetrical tyrosination) can lead to a non-mendelian selection of stronger centromeres (higher kinetochore protein). In cases where the weaker centromere is located on the central side of the spindle, the K-MT attachments are degraded and reform to bring the stronger centromere towards the center of the cell. Importantly, peripheral GV oocytes that displayed a correction mechanism by relocating their GVs to the center (before spindle assembly) had a significant decrease in the percentage of abnormal K-MT attachments when compared to uncorrected oocytes. Taken together, these findings suggest that primary spindle formation and positioning in the center of the oocyte may serve as an essential protection mechanism against cortical signals capable of influencing improper K-MT attachments.

Germinal vesicle positioning is often studied only *in vitro* or at a single time point *in vivo* and is thus not very well understood. There has been a long-standing debate regarding the position of the GV in mammalian oocytes. For example, a previous study found that the majority of prophase I-arrested oocytes have peripherally located GVs, and this cortical positioning of the GV is likely influenced by gap junctions and increased cumulus cell contact (Barrett and Albertini, 2010). On the other hand, other studies demonstrated that the majority of prophase I-arrested oocytes have centrally positioned GVs (Almonacid, et al., 2019, Brunet and Maro, 2007, Levi, et al., 2013). Interestingly, in the first study (Barrett and Albertini, 2010), the oocytes were collected from mice aged 21 days, whereas in the other studies (Almonacid, Al Jord, El-Hayek, Othmani, Coulpier, Lemoine, Miyamoto, Grosse, Klein, Piolot, Mailly, Voituriez, Genovesio and Verlhac, 2019, Brunet and Maro, 2007, Levi, Ghetler, Shulman and Shalgi, 2013), the

oocytes were collected from mice aged above 8-week old. Our results that the majority of oocytes collected from 2-3-week old mice exhibited a peripherally located GVs and that the majority of oocytes collected from 6-8-week old mice exhibited a centrally located GVs clearly explained the previous findings and add greater clarity to the field. However, why and how GV positioning is a dynamic process during oocyte development remains unknown. During oocyte meiosis, prophase I-arrested oocytes have a cytoplasmic mesh of F-actin vesicles that experience increased movement near the cortex and decreased movement near the center (Almonacid, Terret and Verlhac, 2014). Accordingly, the gradient of F-actin creates a gentle force that encourages the GV to position in the center of the cell through active diffusion (Almonacid, et al., 2018). Analyzing the cytoskeletal changes within the oocyte during its development and growth may reveal more insight into the underlying mechanisms behind GV positioning throughout oogenesis.

Current *in vitro* fertilization (IVF) technologies maintain much room for improvement, as only 12.7% of naturally ovulated IVF cycles in humans produce a pregnancy and only 8.8% of those pregnancies result in live births (Nargund, et al., 2001). Although technologies and protocols have advanced since the first IVF birth in 1978, the success rate in producing a live birth in women under the age of 35 through IVF remains less than 50% (Technology, 2019). To date, there are no definitive morphological markers of predictive oocyte quality and successful IVF that are particularly non-invasive (Rienzi, et al., 2011). Understanding the association between peripherally located GV and the incidence of aneuploidy may allow for the selection of oocytes predisposed to correct segregation of chromosomes. Additionally, arresting the cell and enabling the GV to relocate to central positioning may be a promising approach to increase the overall

efficacy of IVF practices, allowing for increases in blastocyst rate, pregnancy rate, and live birth rate in all species.

MATERIAL AND METHODS

Ethics

All laboratory animals were managed, and experiments conducted, in compliance with the University of Missouri (Animal Care Quality Assurance Reference Number, 9695).

Oocyte collection and in vitro *maturation (IVM)*

Full-grown GV oocytes were collected from CF-1 female mice aged 6-8 weeks. Oocyte collection and culture were carried out as previously described (Balboula and Schindler, 2014, Stein and Schindler, 2011). Cumulus oocyte complexes (COCs) were collected and cultured in bicarbonate-free minimal essential medium (MEM) supplemented with 3mg/ml polyvinylpyrrolidone (PVP) and 25 mM Hepes (pH 7.3) under mineral oil (MilliporeSigma, St. Louis, MO, USA # M4659, # P2307, # H3784, # M8410). Oocytes were manually denuded and sorted into 3 groups: Central GV, Intermediate GV, Peripheral GV. Careful rolling of the oocyte ensured correct classification. Oocytes were then transferred to Chatot, Ziomek, and Bavister (CZB) medium (Chatot, et al., 1989) supplemented with 1µM glutamine (MilliporeSigma, # G8549) under mineral oil and matured at 37˚C with humidified 5% CO_2 in an incubator for either 7, 14, or 16 h.

Nocodazole (Sigma #M1404) and ZM447439 (Tocris #2458) were dissolved in dimethyl sulfoxide (DMSO) and added to CZB culture medium at a final concentration of 5µm and 10µm, respectively.

275 ***Immunocytochemistry***

276 After maturation, oocytes were fixed in a freshly prepared solution of 2.5% (kinetochore
277 experiments) or 3.7% (morphology experiments) paraformaldehyde (MilliporeSigma, # P6148)
278 dissolved in phosphate buffer saline (PBS). Oocytes were incubated in permeabilization solution
279 (0.1% Triton X-100 in PBS) for 20 minutes and blocking solution (0.3% BSA and 0.01%
280 Tween-20 in PBS) for 20 minutes before staining. Oocytes were incubated at room temperature
281 for one h with the primary antibody before undergoing 3 consecutive washes in blocking solution
282 for 9 minutes each. Oocytes were then incubated at room temperature for one h in the secondary
283 antibody solution. Following another 3 consecutive washes in blocking solution at 9 minutes
284 each, oocytes were mounted on glass slides using Vectashield containing 4',6-Diamidino-2-
285 Phenylindole, Dihydrochloride (DAPI; Vector Laboratories, Burlingame, CA, USA) in order to
286 stain the DNA. Fluorescence was observed using a 40X oil objective using a Leica DMI8
287 microscope and oocytes were imaged using 3 µm Z-intervals. Oocytes were analyzed using NIH
288 ImageJ software (National Institute of Health, Bethesda, MD USA).
289 The following primary antibodies were used in immunofluorescence: conjugated α-tubulin-
290 AlexaFluor 488 (Life Technologies # 322 588; 1:75), CREST autoimmune serum (Antibodies
291 Incorporated # 15-234; 1:25).
292
293 ***In situ chromosome counting***
294 Oocytes matured *in vitro* for 14 h in CZB medium supplemented with L-glutamine under mineral
295 oil were transferred to CZB containing 100 µm monastrol (MilliporeSigma, # M8515) and
296 incubated an extra 2 h; monastrol is an Eg5-kinesin inhibitor which induces monopolar spindle
297 formation and thus results in a rosette of chromosome distribution (Balboula and Schindler,

2014, Duncan, et al., 2009). After treatment with monastrol, oocytes at Met II stage were fixed in a freshly prepared solution of 2.5% paraformaldehyde (MilliporeSigma, # P6148) and stained with CREST autoimmune serum (Antibodies Incorporated # 15-234; 1:25) to label the kinetochores. DAPI was used to label the DNA. Fluorescence was observed using a 40X oil objective using a Leica DMI8 microscope and oocytes were imaged using 0.5 µm Z-intervals in order to observe all kinetochores. Oocytes were analyzed individually and were scored either as euploid (containing 40 kinetochores) or as aneuploid (containing ± 40 kinetochores).

Assessment of kinetochore-microtubule attachment

Cells were matured *in vitro* for 7 h in CZB medium supplemented with L-glutamine under mineral oil. The oocytes were placed on ice for 6 minutes in a 96 well dish containing chilled MEM. Exposing the oocytes to cold shock depolymerizes unattached MTs; however, when MTs have established end-on attachment to a kinetochore, it becomes cold stable (Rieder, 1981). Oocytes were fixed using a freshly prepared 2.5% paraformaldehyde solution and immunostained with anti-human CREST (to label kinetochores) and α-tubulin (to label MTs) antibodies. DAPI was used to label DNA. Cells were imaged using a Leica TCS SP8 confocal microscope and a x63 oil objective, taking images at 0.5 µm Z-intervals. Kinetochores were analyzed for unattached, normal, or abnormal attachments (syntelic - both kinetochores attached to one side of the spindle or merotelic - a kinetochore maintaining attachment to both sides of the spindle). Oocytes were analyzed using NIH ImageJ Software.

321 ***Time-lapse microscopy***

322 Full-grown oocytes collected from CF-1 mice aged 6-8 weeks were imaged once every 30
323 minutes over time using a 40X oil objective on a Leica DMI8 microscope within a
324 microenvironmental chamber maintaining an atmosphere of 5% CO_2 and temperature of 37˚C in
325 humidified air. DIC imaging acquisition began before NEBD, capturing images at 5 µm Z-
326 intervals with minimal light exposure and intensity. Image sequences were analyzed using NIH
327 ImageJ Software.

328

329 ***Oocyte histology***

330 Ovaries from CF-1 mice of varying ages (2 weeks, 3 weeks, 5 weeks, and 8 weeks) were
331 collected, submerged, and stored in buffered zinc formalin overnight. Tissues were then moved
332 to 70% ethanol for storage until undergoing a 10-h protocol using a Leica ASP300S enclosed
333 tissue processor. After processing, tissues were embedded in paraffin wax and cooled fully using
334 the Leica EG1150 C/H pair. Embedded tissues were sectioned at 8 µm thickness using a Leica
335 Histocore AutoCut microtome. Representative samples were taken for each age by taking 3
336 consecutive sections periodically (every 4, 6, 8, or 10 sections respectively). Tissues were
337 stained with Hematoxylin and Eosin (ABCAM, # 245880) before being mounted with permount
338 resin (Thermo Fisher Scientific, Inc. # SP15). Oocytes and their corresponding GV positioning
339 were examined using a 10X objective on a Leica DMI8 microscope.

340

341 ***Statistical analysis***

342 Tests used to evaluate the statistical significance of the findings reported include One-way
343 ANOVA, Student t-test, and chi-square contingency testing within GraphPad Prism. The Tukey

post hoc test was utilized to determine statistical significance between groups. P values of < 0.05 were considered significant. All data are displayed as means ± SEM.

Declaration of interest

All authors declare that there are no conflicts of interest that may prejudice or bias the research reported.

Funding

This research was supported by laboratory start-up funding from the University of Missouri to AZB.

Acknowledgements

The authors would like to thank all members of the Balboula lab at the University of Missouri, Columbia for dedicated help and encouragement. The authors would like to thank Heide Schatten, Pramod Dhakal, Rocio Rivera, Thomas Spencer, Yuksel Agca, and the Molecular Cytology Core for equipment usage and valuable discussion.

Figure Legends

Figure 1: Germinal vesicle positioning is a dynamic process throughout the development

(A) Full-grown oocytes were collected, imaged and classified into one of three groups: central germinal vesicle (GV), intermediate GV, or peripheral GV according to the distance measured from the GV to the nearest cortex (B) Quantification of the average distance from the GV to the nearest cortex within groups established in “A”. One-way ANOVA and Tukey’s post hoc test

were performed to analyze the data. (C) Representative images of oocytes with a central, intermediate, and peripherally located GV. The scale bars represent 100 µm. (D) Quantification of the contribution of each group to all oocytes as collected in "C". One-way ANOVA and Tukey's post hoc test were performed to analyze the data. (E) Histological analysis of GV positioning *in vivo* at different ages. Ovaries from 2, 3, 5, and 8 weeks old mice were collected, fixed, and stained with Hematoxylin and Eosin. Sections were observed through 10X and 40X objective magnification and classified into one of the three positioning groups: central, intermediate, peripheral. The scale bar represents 100 µm. (F) Representative images of GV positioning in 3 and 8 weeks old mice. The white box emphasizes the location of the magnified image within the ovary. The scale bar represents 100 µm. (G) Quantification of the proportion of oocytes sorted according to their GV positioning (central, intermediate, peripheral) in 2, 3, 5, and 8 week old mice. Two-way ANOVA and Sidak's multiple comparison test were performed to determine if the groups differed significantly. Data are displayed as mean ± SEM. Values with asterisks vary significantly, * $P < 0.05$, ** $P < 0.01$, *** $P < 0.001$, **** $P < 0.0001$. The total number of analyzed oocytes (from at least 3 independent replicates) is specified above each graph.

Figure 2: Oocytes with a peripherally located germinal vesicle have higher rates of chromosome misalignment and aneuploidy.

Full-grown prophase I oocytes were collected and sorted into central, intermediate and peripheral groups based on germinal vesicle (GV) positioning and imaged live using time-lapse microscopy during *in vitro* maturation for 16 h (Met II). (A) Quantification of the percentage of oocytes underwent NEBD. (B) Quantification of the average time of NEBD. (C) Quantification of the

390 percentage of first polar body extrusion (1st PBE). (D) Quantification of the average time of
391 PBE. (E-J) Full-grown prophase I oocytes were collected and sorted into central, intermediate
392 and peripheral groups based on GV positioning and *in vitro* matured for 7 h (Met I) or 16 h (Met
393 II. Oocytes were fixed and immunostained with a-tubulin to label the spindle. DNA was labeled
394 by DAPI. (E) Representative confocal images of Met I oocytes. (F) Quantification of the
395 percentage of chromosome misalignment in Met I oocytes. (G) Quantification of the percentage
396 of abnormal spindle morphology in Met I oocytes. (H) Representative confocal images of Met II
397 oocytes. (I) Quantification of the percentage of chromosome misalignment in Met II oocytes. (J)
398 Quantification of the percentage of abnormal spindle morphology in Met II oocytes. (K) Full-
399 grown prophase I oocytes were collected and sorted into central, intermediate and peripheral
400 groups based on GV positioning and *in vitro* matured for 14 h (Met II). Oocytes were fixed and
401 immunostained with CREST antibody to label kinetochores. DNA was labeled by DAPI.
402 Oocytes were analyzed individually and scored either as euploid (containing 40 kinetochores) or
403 as aneuploid (containing ± 40 kinetochores). Shown are representative images. (L)
404 Quantification of the percentage of aneuploid eggs. The scale bar represents 10 μm. One-way
405 ANOVA and Tukey's post hoc tests were performed to determine statistical significance among
406 groups. Data are displayed as mean ± SEM. Values with asterisks vary significantly, * $P < 0.05$,
407 ** $P < 0.01$, *** $P < 0.001$. The total number of analyzed oocytes (from at least 3 independent
408 replicates) is specified above each graph.
409
410
411

Figure 3: Cortically located germinal vesicle favor central movement, but experience NEBD during relocation

(A) Representative images of time-lapse microscopy of the movement of peripherally located germinal vesicle (GV) during prophase I arrest. Images were taken every 10 minutes using a Z-interval of 0.5 µm (see Supplemental Movie 1). The black circle identifies the initial GV position, while the green circle identifies the final GV position. The scale bar represents 50 µm. (B) Quantification of the percentage of GV relocation to a central position in intermediate and peripheral oocytes. (C-F) Full-grown prophase I oocytes were collected and sorted into central, intermediate and peripheral groups based on germinal vesicle (GV) positioning and imaged live using time-lapse microscopy during *in vitro* maturation. (C) Quantification of the change in the distance of GV to the nearest cortex (from the initial position at the GV stage to the final destination at NEBD). (D) Quantification of the change in the distance of chromosomes to the cortex (from NEBD until all chromosomes aligned). (E) Quantification of the average time of chromosome alignment. (F) Quantification of the change in the distance of chromosomes to the cortex (from the initial position at the GV stage to the final destination when chromosomes aligned). Alignment, and PBE. One-way ANOVA and Tukey's post hoc test were performed to determine statistical significance. Data are displayed as mean ± SEM. Values with asterisks vary significantly, * $P < 0.05$, ** $P < 0.01$, *** $P < 0.001$, **** $P < 0.0001$. The total number of analyzed oocytes (from at least 3 independent replicates) is specified above each graph.

Figure 4: Oocytes with peripherally located germinal vesicle experience higher levels of incorrect kinetochore-microtubule attachments

(A) Full-grown prophase I oocytes were collected and sorted into central, intermediate and peripheral groups based on germinal vesicle (GV) positioning followed by *in vitro* maturation in milrinone-free medium in the presence of nocodazole. Randomly selected oocytes were *in vitro* matured in the presence of nocodazole and ZM447439 (positive control group). The percentage of polar body extrusion (PBE) was assessed at 16 h (Met II). (B) Representative images of kinetochore-microtubule attachments in oocytes with a central, intermediate, or peripherally located GV. Panels on the right (from top to bottom) display normal K-MT attachment, unattached kinetochores and abnormal K-MT attachment. (C) Quantification of the percentage of unattached kinetochores, normal K-MT attachments (D), and abnormal K-MT attachments (E). (F) Quantification of the oocytes with 2 or more incorrect K-MT attachments. One-way ANOVA and Tukey's post hoc test were performed to analyze the data. Data are displayed as mean ± SEM. Values with asterisks vary significantly, * $P < 0.05$, ** $P < 0.01$, **** $P < 0.0001$. The total number of analyzed oocytes (from at least 3 independent replicates) is specified above each graph.

Figure 5: Relocation of the germinal vesicle decreases the incidence of aneuploidy in peripheral germinal vesicle oocytes

(A) Schematic depicting the determination of corrected, migratory, and peripheral oocytes. (B) Full-grown oocytes with peripherally located germinal vesicle (GV) were collected and imaged live during *in vitro* maturation using time-lapse microscopy. (B) Representative images of the GV movement prior to NEBD. Images were taken every 30 minutes (Z-interval of 5 µm) to

457 minimize light exposure and intensity. The black circle denotes the primary GV positioning,
458 while the green circle denotes the final GV position prior to NEBD. (C) Quantification of the
459 incidence of aneuploidy in metaphase II oocytes from the oocytes categorized in B. One-way
460 ANOVA and Tukey's post hoc test were performed to determine any statistical significance.
461 Data are displayed as mean ± SEM. Values with asterisks vary significantly, * $P < 0.05$. The total
462 number of analyzed oocytes (from at least 3 independent replicates) is specified above each
463 graph.
464
465 **Supplementary Movie 1:** Time-lapse microscopy of germinal vesicle (GV) oocytes cultured in
466 milrinone-containing medium to induce prophase I arrest. DIC images were captured every 10
467 minutes at Z-intervals of 5 µm. The scale bar represents 50 µm.
468
469 **Supplementary Movie 2:** Time-lapse microscopy of peripheral germinal vesicle (GV) oocyte
470 showing corrected GV relocation during *in vitro* maturation (Same oocyte used in the top panels
471 of Fig. 5B). DIC images were captured every 10 minutes at Z-intervals of 5 µm. The scale bar
472 represents 50 µm.
473
474 **Supplementary Movie 3:** Time-lapse microscopy of peripheral germinal vesicle (GV) oocyte
475 showing migratory GV relocation during *in vitro* maturation (Same oocyte used in the middle
476 panels of Fig. 5B). DIC images were captured every 10 minutes at Z-intervals of 5 µm. The scale
477 bar represents 50 µm.
478

479 **Supplementary Movie 4:** Time-lapse microscopy of peripheral germinal vesicle (GV) oocyte
480 that failed to relocate its GV during *in vitro* maturation (Same oocyte used in the lower panels of
481 Fig. 5B). DIC images were captured every 10 minutes at Z-intervals of 5 µm. The scale bar
482 represents 50 µm.

483

484 # REFERENCES

Akera T, Chmatal L, Trimm E, Yang K, Aonbangkhen C, Chenoweth DM, Janke C, Schultz RM, Lampson MA. Spindle asymmetry drives non-Mendelian chromosome segregation. *Science* 2017;358: 668-672.

Almonacid M, Ahmed WW, Bussonnier M, Mailly P, Betz T, Voituriez R, Gov NS, Verlhac MH. Active diffusion positions the nucleus in mouse oocytes. *Nat Cell Biol* 2015;17: 470-479.

Almonacid M, Al Jord A, El-Hayek S, Othmani A, Coulpier F, Lemoine S, Miyamoto K, Grosse R, Klein C, Piolot T *et al.* Active Fluctuations of the Nuclear Envelope Shape the Transcriptional Dynamics in Oocytes. *Dev Cell* 2019;51: 145-157 e110.

Almonacid M, Terret ME, Verlhac MH. Actin-based spindle positioning: new insights from female gametes. *J Cell Sci* 2014;127: 477-483.

Almonacid M, Terret ME, Verlhac MH. Control of nucleus positioning in mouse oocytes. *Semin Cell Dev Biol* 2018;82: 34-40.

Angell RR, Templeton AA, Aitken RJ. Chromosome studies in human in vitro fertilization. *Hum Genet* 1986;72: 333-339.

Azoury J, Lee KW, Georget V, Rassinier P, Leader B, Verlhac MH. Spindle positioning in mouse oocytes relies on a dynamic meshwork of actin filaments. *Curr Biol* 2008;18: 1514-1519.

Balboula AZ, Nguyen AL, Gentilello AS, Quartuccio SM, Drutovic D, Solc P, Schindler K. Haspin kinase regulates microtubule-organizing center clustering and stability through Aurora kinase C in mouse oocytes. *J Cell Sci* 2016;129: 3648-3660.

Balboula AZ, Schindler K. Selective disruption of aurora C kinase reveals distinct functions from aurora B kinase during meiosis in mouse oocytes. *PLoS Genet* 2014;10: e1004194.

Balboula AZ, Stein P, Schultz RM, Schindler K. RBBP4 regulates histone deacetylation and bipolar spindle assembly during oocyte maturation in the mouse. *Biol Reprod* 2015;92: 105.

Barrett SL, Albertini DF. Cumulus cell contact during oocyte maturation in mice regulates meiotic spindle positioning and enhances developmental competence. *J Assist Reprod Genet* 2010;27: 29-39.

Brunet S, Maro B. Germinal vesicle position and meiotic maturation in mouse oocyte. *Reproduction* 2007;133: 1069-1072.

Byrne J, Warburton D, Kline J, Blanc W, Stein Z. Morphology of early fetal deaths and their chromosomal characteristics. *Teratology* 1985;32: 297-315.

Chatot CL, Ziomek CA, Bavister BD, Lewis JL, Torres I. An improved culture medium supports development of random-bred 1-cell mouse embryos in vitro. *J Reprod Fertil* 1989;86: 679-688.

Duncan FE, Chiang T, Schultz RM, Lampson MA. Evidence that a defective spindle assembly checkpoint is not the primary cause of maternal age-associated aneuploidy in mouse eggs. *Biol Reprod* 2009;81: 768-776.
Gilbert S. Oogenesis *Developmental Biology*. 2000. Sinauer Associates, Inc, Sunderland, Massachusetts.
Gruhn JR, Zielinska AP, Shukla V, Blanshard R, Capalbo A, Cimadomo D, Nikiforov D, Chan AC, Newnham LJ, Vogel I *et al.* Chromosome errors in human eggs shape natural fertility over reproductive life span. *Science* 2019;365: 1466-1469.
Hassold T, Hall H, Hunt P. The origin of human aneuploidy: where we have been, where we are going. *Hum Mol Genet* 2007;16 Spec No. 2: R203-208.
Hassold T, Hunt P. To err (meiotically) is human: the genesis of human aneuploidy. *Nat Rev Genet* 2001;2: 280-291.
Jacobs PA, Baikie AG, Court Brown WM, Strong JA. The somatic chromosomes in mongolism. *Lancet* 1959;1: 710.
Lane M, Bavister BD, Lyons EA, Forest KT. Containerless vitrification of mammalian oocytes and embryos. *Nat Biotechnol* 1999;17: 1234-1236.
Lane SI, Chang HY, Jennings PC, Jones KT. The Aurora kinase inhibitor ZM447439 accelerates first meiosis in mouse oocytes by overriding the spindle assembly checkpoint. *Reproduction* 2010;140: 521-530.
Lane SI, Yun Y, Jones KT. Timing of anaphase-promoting complex activation in mouse oocytes is predicted by microtubule-kinetochore attachment but not by bivalent alignment or tension. *Development* 2012;139: 1947-1955.
Lejeune J, Turpin R, Gautier M. [Mongolism; a chromosomal disease (trisomy)]. *Bull Acad Natl Med* 1959;143: 256-265.
Levi M, Ghetler Y, Shulman A, Shalgi R. Morphological and molecular markers are correlated with maturation-competence of human oocytes. *Hum Reprod* 2013;28: 2482-2489.
Longo FJ, Chen DY. Development of cortical polarity in mouse eggs: involvement of the meiotic apparatus. *Dev Biol* 1985;107: 382-394.
Ma J, Zeng F, Schultz RM, Tseng H. Basonuclin: a novel mammalian maternal-effect gene. *Development* 2006;133: 2053-2062.
McCarthy EK, Goldstein B. Asymmetric spindle positioning. *Curr Opin Cell Biol* 2006;18: 79-85.
Menezo YJ. Paternal and maternal factors in preimplantation embryogenesis: interaction with the biochemical environment. *Reprod Biomed Online* 2006;12: 616-621.
Nargund G, Waterstone J, Bland J, Philips Z, Parsons J, Campbell S. Cumulative conception and live birth rates in natural (unstimulated) IVF cycles. *Hum Reprod* 2001;16: 259-262.
Orr B, Godek KM, Compton D. Aneuploidy. *Curr Biol* 2015;25: R538-542.
Rieder CL. The structure of the cold-stable kinetochore fiber in metaphase PtK1 cells. *Chromosoma* 1981;84: 145-158.
Rienzi L, Vajta G, Ubaldi F. Predictive value of oocyte morphology in human IVF: a systematic review of the literature. *Hum Reprod Update* 2011;17: 34-45.
Sanfins A, Lee GY, Plancha CE, Overstrom EW, Albertini DF. Distinctions in meiotic spindle structure and assembly during in vitro and in vivo maturation of mouse oocytes. *Biol Reprod* 2003;69: 2059-2067.

Sanfins A, Plancha CE, Overstrom EW, Albertini DF. Meiotic spindle morphogenesis in in vivo and in vitro matured mouse oocytes: insights into the relationship between nuclear and cytoplasmic quality. *Hum Reprod* 2004;19: 2889-2899.
Schuh M, Ellenberg J. Self-organization of MTOCs replaces centrosome function during acentrosomal spindle assembly in live mouse oocytes. *Cell* 2007;130: 484-498.
Stein P, Schindler K. Mouse oocyte microinjection, maturation and ploidy assessment. *J Vis Exp* 2011.
Sun H, Gong TT, Jiang YT, Zhang S, Zhao YH, Wu QJ. Global, regional, and national prevalence and disability-adjusted life-years for infertility in 195 countries and territories, 1990-2017: results from a global burden of disease study, 2017. *Aging (Albany NY)* 2019;11: 10952-10991.
Technology SfAR. SART National Summary Report 2017. 2019.

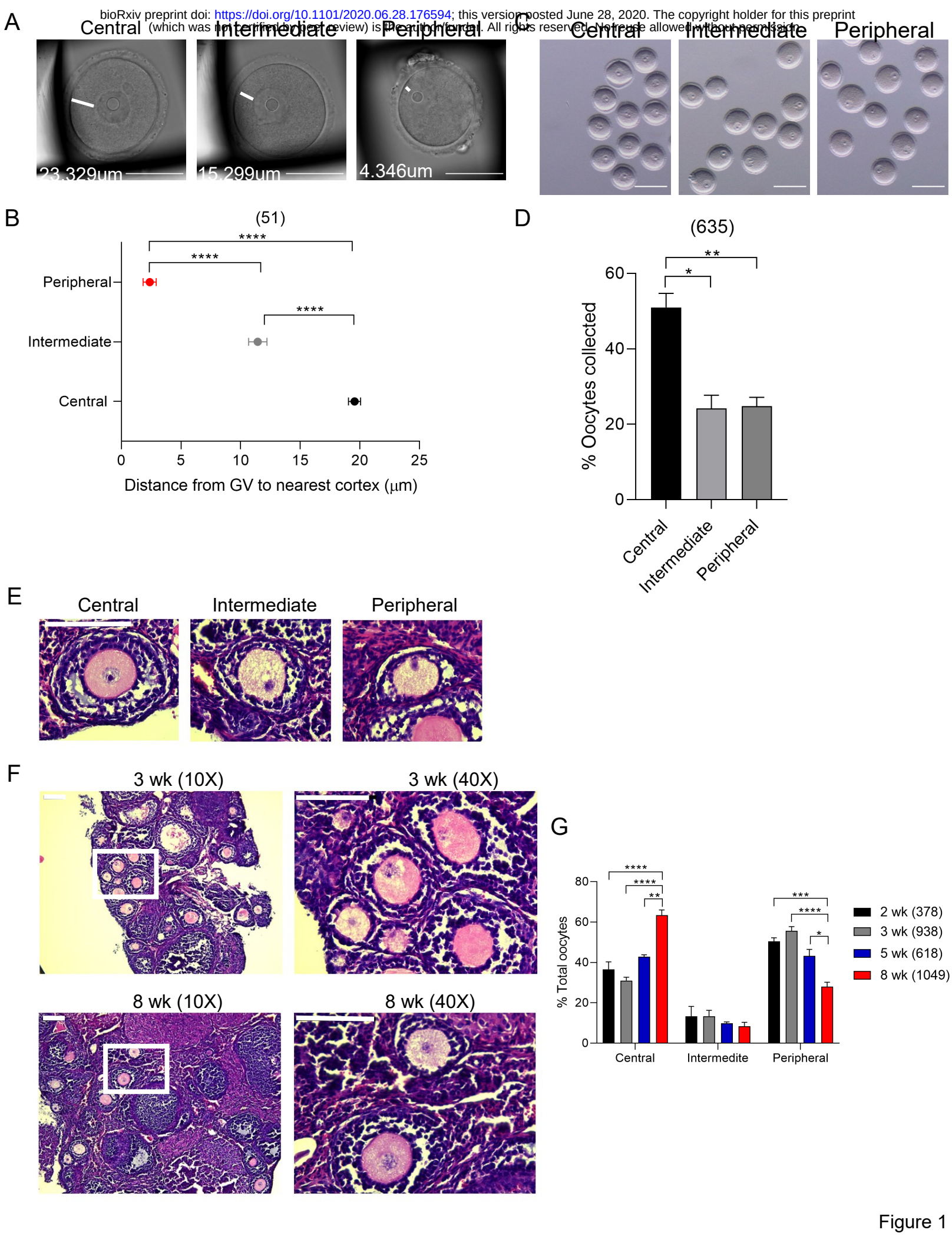

Figure 1

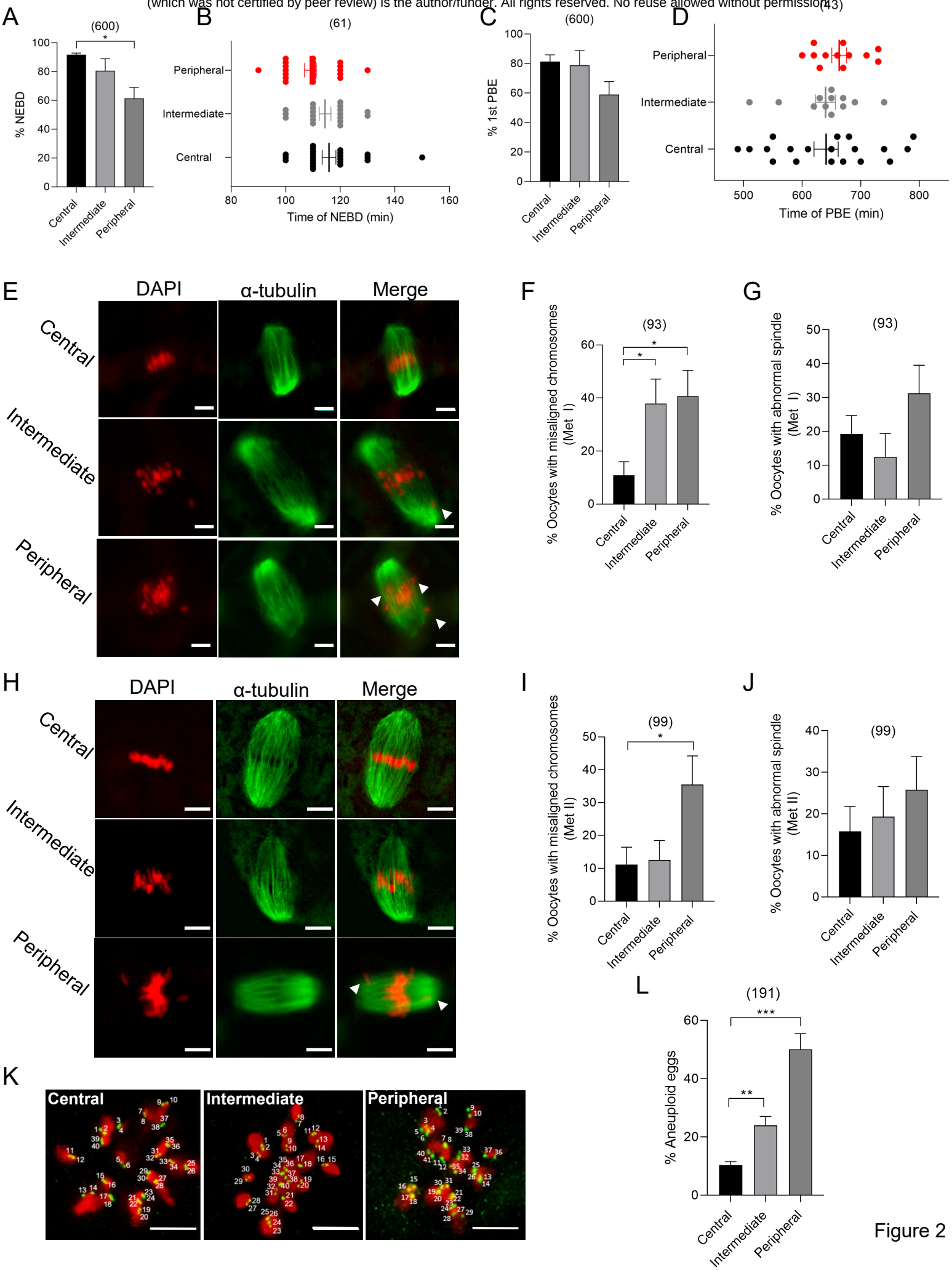

Figure 2

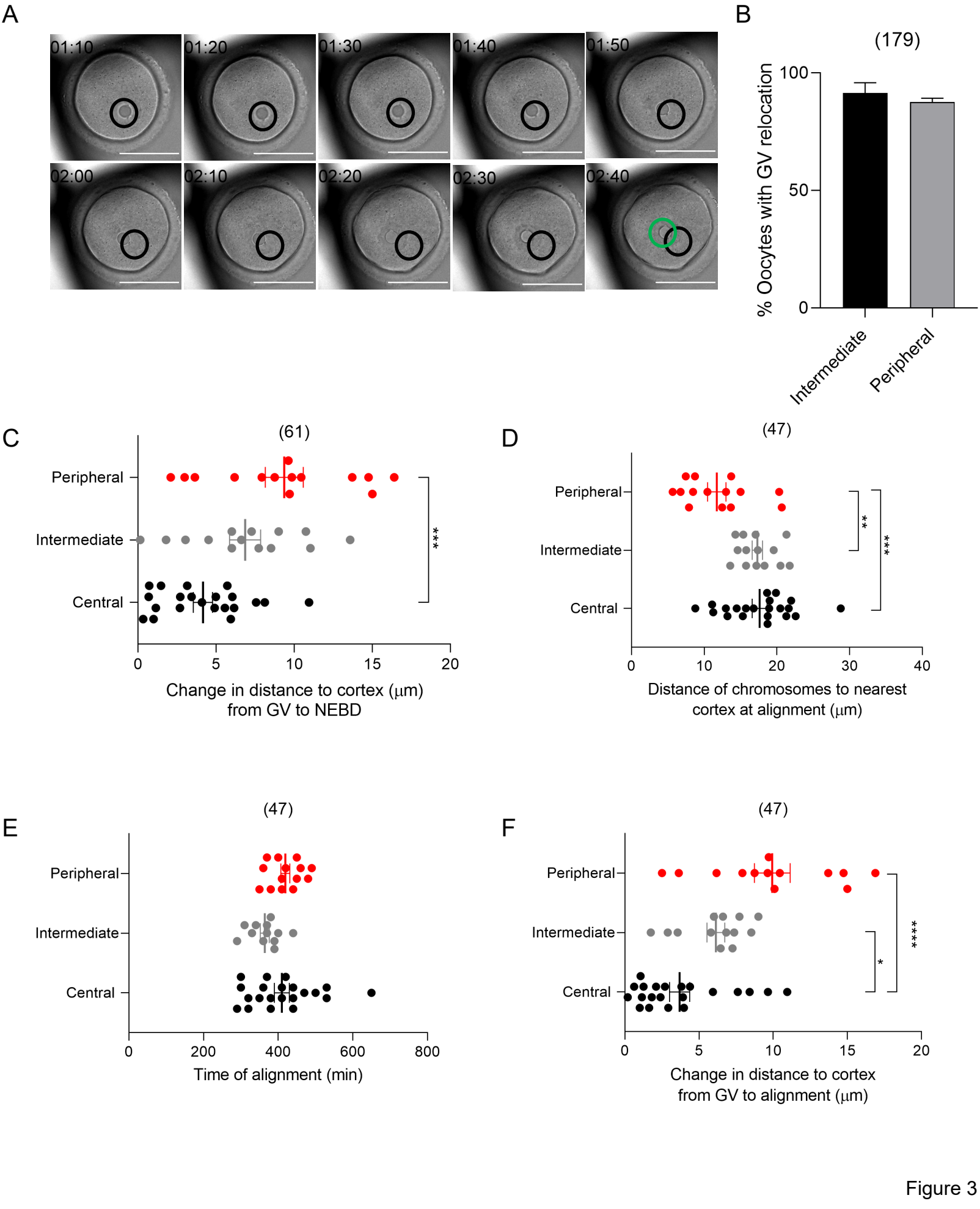

Figure 3

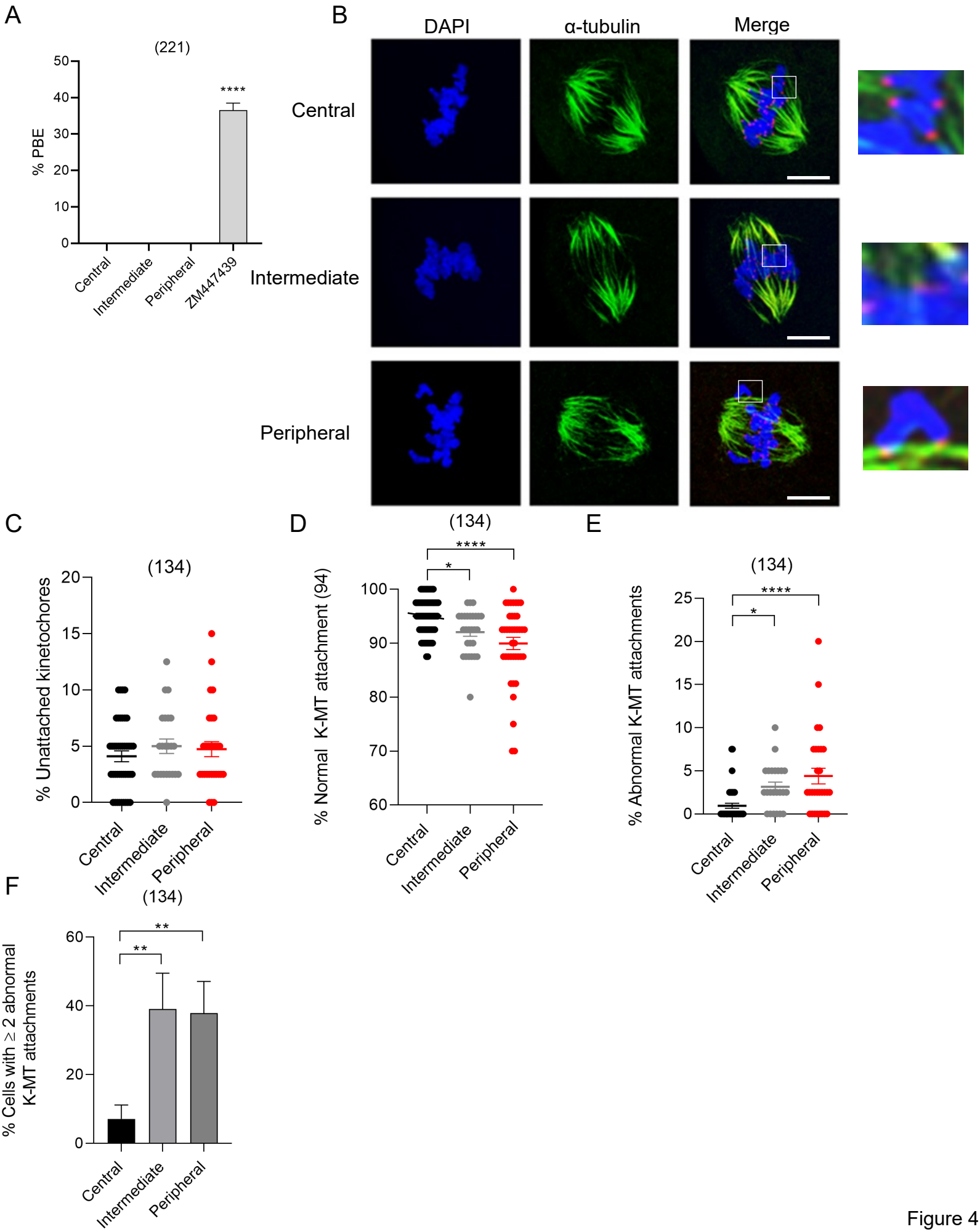

Figure 4

A

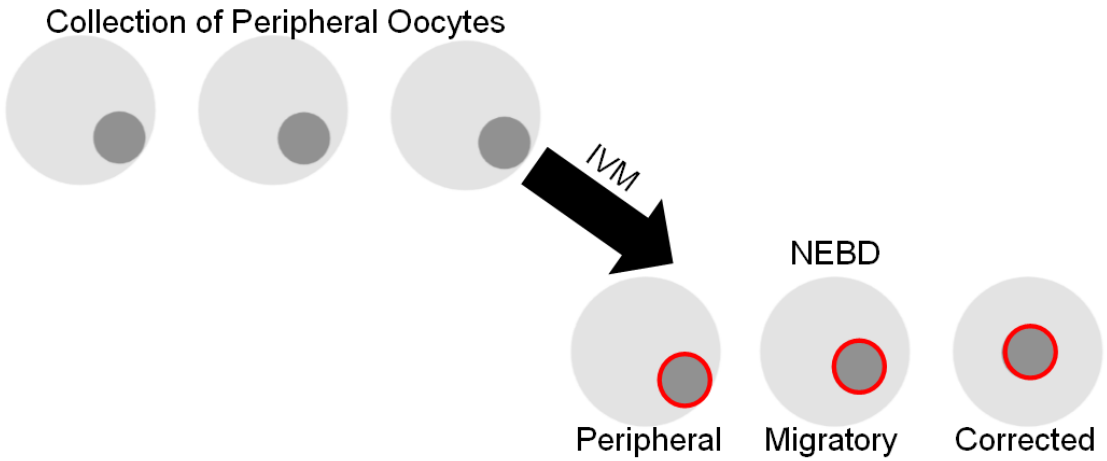

B

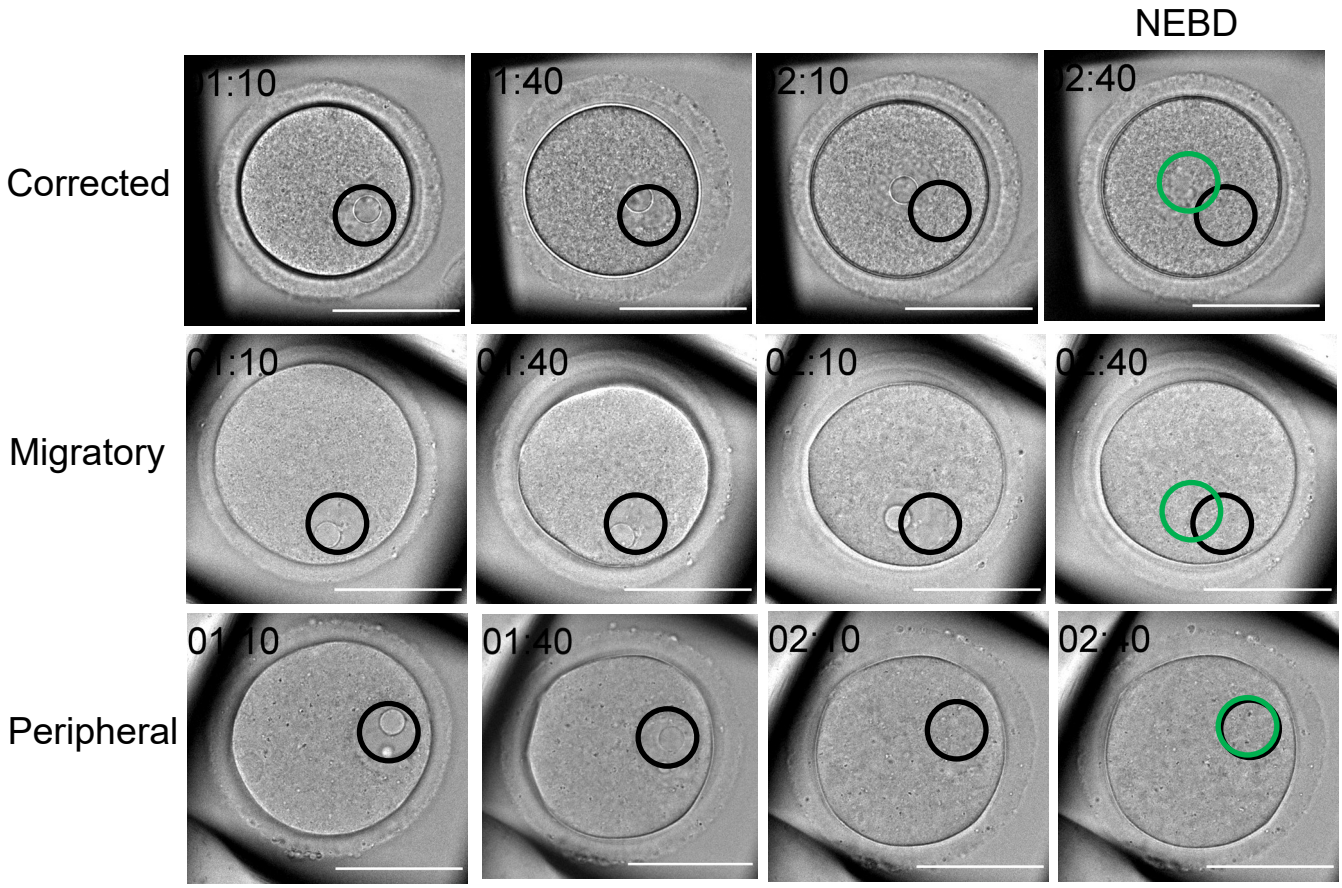

C

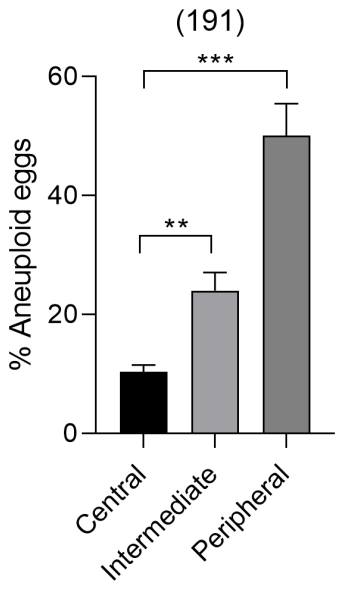

Figure 5